16-4-2019

An Innovative Energy Harvesting Shock Absorber System using Cable Transmission

José Luis Olazagoitia

Lincoln Bowen

Jordi Viñolas

Javier Echávarri Otero

An Innovative Energy Harvesting Shock Absorber System using Cable Transmission

Bowen L[1]., Vinolas J.[1], Olazagoitia J.L[1*], Echávarri Otero J.[2]

Abstract- **This paper presents an innovative design of an energy harvesting shock absorber using cable transmission called Cable-Dynamics Energy Harvesting Shock Absorber (CD-EHSA). It includes the design, modelling, bench experiments, and road tests results. Experimental tests are carried out with the CD-EHSA system in a MTS 835 machine, in order to analyze its behavior and validate the computational model of the CD-EHSA with the tests carried out on the actual component. Likewise, the paper presents the results of recovered electric power by the system during road tests at a speed between 20-30 Km/h. With four CD-EHSA installed in a Renault Twizy, an average power of 105W and power peaks of 400-500W when passing through speed bumps are obtained. The designed system mechanical can reach an efficiency around 60%.**

Keywords: **Energy Harvesting, vehicle suspension, Multi-Objective Optimization Techniques, Simscape, Electromagnetic actuator.**

I. INTRODUCTION

With the proliferation of electric and hybrid cars, in recent decades new lines of research have been opened for technologies used in the recovery of thermal and mechanical energy in automobiles [1]. An example of the type of technology that can be found on the market today is the Kinetic Recovery System (KERS). Its operation consists of recovering the kinematic energy and as a consequence reduces the demand on friction brakes.
But there are other sources of wasted mechanical energy in the car which have the potential to be recovered. For example F. Khameneifar et al. [2] devised a support on which the engine sits not only able to absorb vibrations, but also recovers part of the energy using piezoelectric materials. Another example is described by J. Lee et al. [3] who uses piezoelectric materials to recover energy from deformations of the wheels. In spite of previous examples though, one of the greatest sources of vibration energy is the vehicle suspension.

The Energy Harvesting Shock Absorber (EHSA), a device which replaces the typical damper and is able to add damping and recover energy at the same time, has been studied by various authors. Different technologies have been used for EHSAs, those that work with piezoelectric materials, such as those proposed by X.D. Xie y/o W. Zhang et al. [4][5], as well as those that operate by electromagnetic principles. M. Abdelkareem et al. [6] resumed very well all this kind of technology that have been presenting in the last ten years.
The electromagnetic EHSA can be classified in two groups: the linear EHSA and the rotational EHSA, or as other authors called: the direct-drive and the indirect-drive.
The linear ones or direct-drive are those that use the same relative translation displacement of the conventional dampers to create a variable magnetic field that allows to induce an electric current, this is the case of E. Asadi and/or X. Tang et al [7][8]. The first one focused on the damping coefficient that could provide his EHSA, giving a range between 1302-1540 Ns/m. The second not only focused on the damping coefficient, but also in the power density generated, giving 3.8 time more compared with L. Zuo design et al. [9].

The rotational or indirect-drive are those which introduce some mechanism to convert translation into rotation and thus are able to use a current rotary generator. The literature offers many examples of rotational EHSA and they have become more popular due to its easy design and construction. Several systems can convert translation into rotation.

First, we have the ball-screw transmission used by G. Zhang et al. [10], he proposed not only an energy-regenerative suspension, but also an active controllers to adequate the damping force. B. Hong et al. [11] also developed a vehicle suspension system with energy harvesting capability using this kind of transmission, he carried out an analytical methodology for the optimal design. On the other hand, W. Salman et al. [12] didn't employ the ball-screw transmission exactly, but instead used a helical gears to increase the efficiency of the system.

Then, we have the rack-pinion system. Many prototypes have been developed using this kind of transmission. One example, is the system developed by Z. Li et al. [13], they presented some road test in which they mentioned that when the vehicle is driven 48 km/h an average power of 19 W are obtained. Later, Z. Li. et al. [14] presented the same prototype, but in this case adding the component called Mechanical Motion Rectifier (MMR). S. Guo et al. [15] compare both system, with and without MMR, taking in consideration ride comfort and road handling. Z. Zhang et al. [16] added to the MMR system supercapacitors in order to extend the battery endurance of an EV.

L. Bowen[1], J. Vinolas[1] and J.L. Olazagoitia[1] are with the Department of Industrial and Automotive Engineering (DIIA). Universidad Antonio de Nebrija. C/Pirineos 55, 28040 – Madrid, (Spain) (e-mail: jolazago@nebrija.es).

J. Echávarri Otero[2] is with the Department of Mechanical Engineering. Universidad Politécnica de Madrid. C/José Abascal 2, 28006 – Madrid, (Spain) (e-mail: jechavarri@etsii.upm.es).

The Hydraulic transmission is based on the kinetic energy that a fluid acquires when moved by a difference of pressure inside a closed system. Avadhany et al. [17] presented one of the first Hydraulic-EHSA, named Genshock. In his work, he studied the electric generation through rotary valves and a turbine. He obtained between 400-1200 W of power with a lineal velocity of 0.762m/s. One of his conclusions was that the selection of the fluid is a key factor in the effective transmission of power from the fluid pressure flow into the rotational motion of a hydraulic motor. Another study presenting this type of technology was proposed by Yuxin Zhang et al [18]. They designed a Hydraulic-EHSA and obtained a power output of 33.4W, with an excitation frequency of 1.67 Hz and an amplitude of 50 mm. J Zou et al. [19] went one step further and included a hydraulic rectifier as the MMR. His prototype was used by M. Abdelkareem et al. [20] to estimate the amount of potential and wasted energy in vehicle suspension system for different types of cars (passenger, bus, truck and off-road vehicle).

Finally, there are other more exotics transmission as can be the "Linkage mechanism" et al. [21], "Two-Leg motion" et al.[22] or using flywheel drive presented by R. Zhang et al.[23].

The objective of the EHSA is not only to recover energy due to oscillations in the suspension, but primarily to guarantee comfort for the passengers, ride handling, i.e. an adequate damping. Two of the main problems of the rotational EHSA presented so far are, first of all, the inertias of their moving parts, which taking into account their translation equivalences can be between 60-120 Kg for each shock absorber. These equivalent masses influence the natural frequencies and the dynamic behavior of the suspension. And secondly the backlash produced in most mechanisms when a change of direction occurs in the transmission.

In this work an innovative design of a rotational EHSA is presented in which the inertias of its moving parts and the phenomenon of backlash are diminished comparing to other prototypes seen from the literature.
To achieve this, it has been decided to use a cable transmission to convert the translation movement into rotation. This type of transmission has been used previously for robotic and/or in biomedical mechanisms [24]. The cable transmissions offers several advantages such as high stiffness, high strength, low friction; they do not leak, do not require surface lubrication and have lightness properties. Two threaded pulleys are used to house the cable, thus ensuring the position of the cable at all times, making it possible to reduce non-linearities, as reported by J. Savall et al. [25] [24]. This prototype has been called Cable Dynamics Energy Harvesting Shock Absorber (CD-EHSA). Another contribution of this work is the study of the cable transmission performance in suspension dynamics.

This paper is structured as follows. In section II the design is introduced and the operation of the CD-EHSA is described. Section III presents the dynamic model with its respective analysis and its mathematical equations. In section IV the results of the experimental tests are outlined and the behavior of the system is analyzed. Section V shows the potential of this type of system for energy recovery using data from a real car. The conclusions together with future lines of research are indicated in section VI.

Nomenclature

p	Pitch of the pulleys.	μ	friction coefficient between the pulley and the cable.
d_e	Distance between the axes of the pulleys.	J_m	Inertia of the motor.
r_p	Radius of the pulleys.	J_{mu}	Inertia of the multiplier.
θ_{s2}	Total mooring angle of the Generator Pulley.	J_{pt2}	Inertia of the second pulley transmission.
θ_{s1}	Total mooring angle of the Driven Pulley.	J_{pt1}	Inertia of the first pulley transmission.
b	Horizontal separation of the cable ties to the mobile skate.	J_{pg}	Inertia of the generator pulley.
T_p	Cable pretensión.	k_{pt}	Pulley transmission ratio.
R_i	Resistance of the generator.	k_{mu}	Multiplier ratio.
L_i	Inductance of the generator.	R_{pg}	Generator pulley radius.
r_c	Radius from section of the cable.	K_{re}	Voltage constant.
E	Elastic modulus Steel.	K_t	Torque constant.
k_c	Cable stiffness coefficient.	c_c	Cable damping coefficient.
ω	Excitation frequency.	F_c	Coulomb friction
F_{brk}	Stribeck friction	F_v	Viscous friction
V_g	Generator voltage	R_e	External electric load

η_g^e	Experimental mechanical efficiency	η_g	Theoretical mechanical efficiency

II. DESIGN AND CONCEPT

The CD-EHSA design presented in Figure 1 is an energy recovery damper which works by cable transmission.

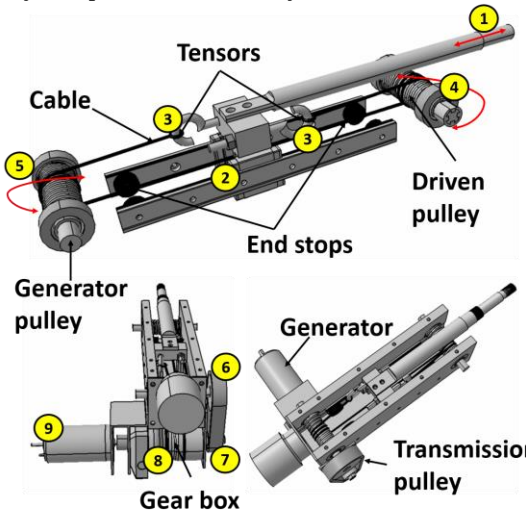

Figure 1. Cad model of the Cable-Dynamics Energy Harvesting Shock Absorber.

The translation movement found in the suspension is transferred by means of a piston (1) to a mobile skate resting on linear guides (2). The skate has two tensioners (3) that pull the cable according to the movement. The cable is wound in two threaded pulleys located at its ends: one pulley (Driven Pulley (4)) has free rotation and the other pulley (Generator Pulley (5)) is coupled to a larger diameter pulley (6). The pulley of greater diameter transmits the movement by means of a band to a smaller pulley (7), in this case the rotational speed is doubled. This last pulley is coupled to a multiplier (8), which in turn is connected to an electric generator (9).

In order to avoid non-linearities in the transmission of the cable, the cable length must always remain constant along the entire travel of the mobile skate. In this way undesired tensions in the cable are prevented, as indicated by J. Savall et al. [26]. To ensure that the length of the cable is always constant, the distance of the tie points d_a, which is indicated in Figure 2, has to fulfill equation (1). This equation is deduced previously by Savall [23].

$$d_a = \left(\frac{d_e - b}{2\pi r_p} + \frac{\theta_{s2}}{2\pi} + \frac{\theta_{s1}}{2\pi}\right) p \qquad (1)$$

where p is the pitch of the pulleys' thread, d_e is the distance between the axes of the pulleys, r_p is the radius of the pulleys, θ_{s2} the total mooring angle of the Generator Pulley, θ_{s1} the total mooring angle of the Driven Pulley and b the horizontal separation of the cable ties to the mobile skate.

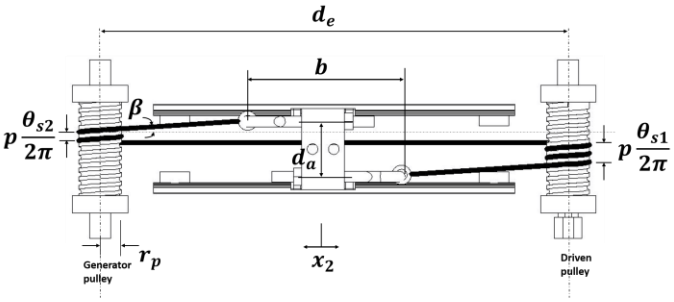

Figure 2. Geometry and main parameters of the cable transmission.

Cable transmissions have been used frequently in all type of industries, in the area of robotics, medical applications, aerospace, etc. Ya-Fei Lu et al. [27] deduce the analytical expression of the maximum torque that the cable can transmit with no slip.

$$M_{max} = 2T_p r_p \frac{\tau_c - 1}{\tau_c + 1} \qquad (2)$$

where T_p is the cable pretension and τ_c is given by equation 3.

$$\tau_c = e^{\mu\theta_{s2}} \qquad (3)$$

μ is the friction coefficient between the pulley and the cable. It is important that this torque is not exceeded by the resistive torque of the generator, otherwise the cable would slide on the pulley and the expected damping would not occur. For this reason, two tensioners have been added on both sides of the skate to vary the pretension of the cable according to the specifications. However, special care must be taken when tensioning the cable because the bearings can be affected by the radial force applied to them.

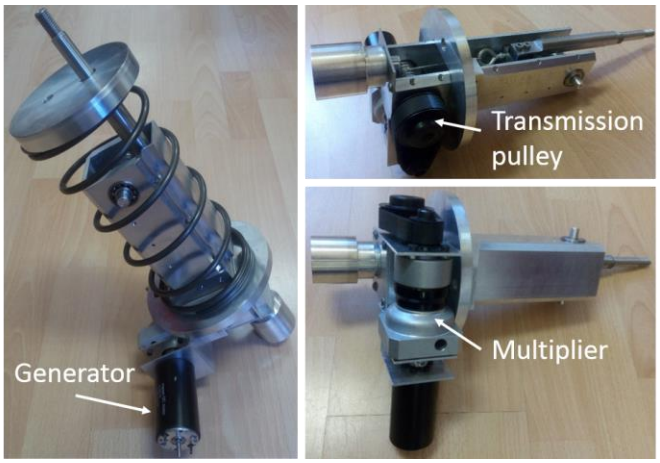

Figure 3. Photo of the shock absorber prototype.

The prototype can be seen in Figure 3. The design parameters of the CD-EHSA, which are listed in Table 1, have been chosen in order to obtain a translation-rotation coefficient of 6 mm/rev. This is a value close to the coefficients used in other EHSA-rotational systems [28][29]. With the generator chosen, a damping coefficient of less than 3500 $N/(m/s)$ can be achieved, which fall within the types of shock absorbers that will be used later.

Table 1. Main characteristics of the Cable Dynamics Energy Harvesting Shock Absorber (CD-EHSA).

Inertia of the motor	J_m	121	gcm^2
Inertia of the multiplier	J_{mu}	100	gcm^2
Inertia of the second pulley transmission	J_{pt2}	8.23	gcm^2
Inertia of the first pulley transmission	J_{pt1}	233	gcm^2
Inertia of the generator pulley	J_{pg}	81	gcm^2
Pulley transmission ratio	k_{pt}	2	
Multiplier ratio	k_{mu}	5	
Generator pulley radius	R_{pg}	10	mm
Voltage constant	K_{re}	0.137	Vs/rad
Torque constant	K_t	0.137	Nm/A
Resistance of the generator	R_i	6.6	Ω
Inductance of the generator	L_i	1.7	mH
Radius from section of the cable	r_c	2	mm
Elastic modulus steel	E	70.3	GPa
Cable stiffness coefficient	k_c	1104	KN/m
Cable damping coefficient	c_c	100	$N/(m/s)$

III. MODELLING AND DYNAMICS

In this section the mathematical equations of the CD-EHSA system for its subsequent dynamic analysis will be derived. The operating scheme presented in Figure 4 is used.

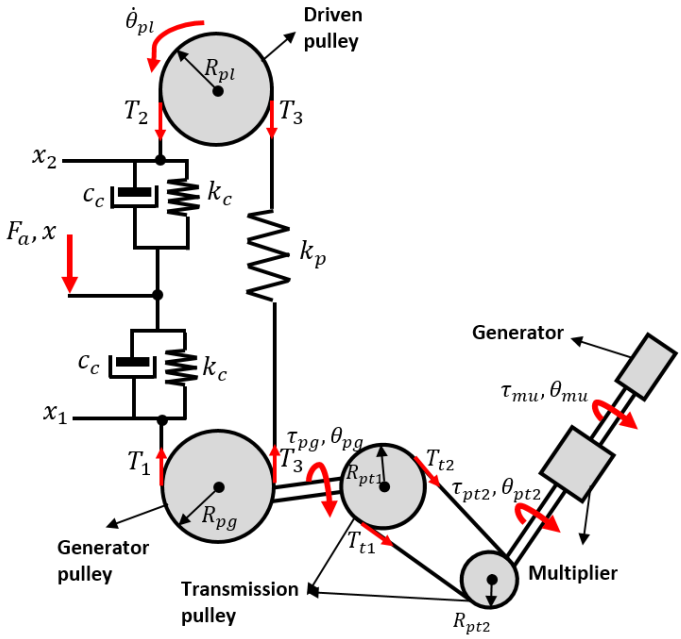

Figure 4. The dynamics model of the proposed Energy-Harvesting Shock Absorber (EHSA).

The dynamic equations of motion of the system presented above are:

$$F_a = T_2 - T_1 \quad (4)$$

$$\eta_{pg}(T_1 - T_3)R_{pg}\dot{\theta}_{pg} = J_{pg}\ddot{\theta}_{pg}\dot{\theta}_{pg} + \tau_{pg}\dot{\theta}_{pg} \quad (5)$$

$$T_1 = k_c(x_1 - x) + c_c(\dot{x}_1 - \dot{x}) \quad (6)$$

$$T_2 = k_c(x - x_2) + c_c(\dot{x} - \dot{x}_2) \quad (7)$$

$$T_3 = k_p(x_2 - x_1) + T_p \quad (8)$$

$$(T_2 - T_1)R_{pl} - J_{pl}\ddot{\theta}_{pl} = 0 \quad (9)$$

$$\dot{\theta}_{pl} = \frac{\dot{x}_2}{R_{pl}} \quad (10)$$

$$\dot{\theta}_{pg} = \frac{\dot{x}_1}{R_{pg}} \quad (11)$$

$$\eta_{pt1}(\tau_{pg}\dot{\theta}_{pg}) = J_{pt1}\ddot{\theta}_{pg}\dot{\theta}_{pg} + (T_{t2} - T_{t1})R_{pt1}\dot{\theta}_{pg} \quad (12)$$

$$\eta_{pt2}(T_{t2} - T_{t1})R_{pt2}\dot{\theta}_{pt2} = J_{pt2}\ddot{\theta}_{pt2}\dot{\theta}_{pt2} + \tau_{pt2}\dot{\theta}_{pt2} \quad (13)$$

$$\eta_{mu}(\tau_{pt2}\dot{\theta}_{pt2}) = J_{mu}(\ddot{\theta}_{mu} - \ddot{\theta}_{pt2})(\dot{\theta}_{mu} - \dot{\theta}_{pt2}) + \tau_g\dot{\theta}_{mu} \quad (14)$$

$$\tau_{mu} = m_r\ddot{\theta}_g + c_r\dot{\theta}_g + k_r\theta_g \quad (15)$$

$$\theta_{mu} = \theta_g \quad (16)$$

$$\frac{R_{pt1}}{R_{pt2}} = \frac{\dot{\theta}_{pt2}}{\dot{\theta}_{pt1}} \quad (17)$$

$$k_{mu} = \frac{\dot{\theta}_{mu}}{\dot{\theta}_{pt2}} \quad (18)$$

$$k_{pt} = \frac{R_{pt1}}{R_{pt2}} \quad (19)$$

The efficiencies ($\eta_{pt1}, \eta_{pt2}, \eta_{mu}$ and η_{pg}) are referring only to the pulley-cable system. From the equations (4) to (11) the force applied to the EHSA is obtained:

$$F_a = \frac{J_{pl}\ddot{\theta}_{pl}}{R_{pl}} + T_3 - \frac{J_{pg}\ddot{\theta}_{pg}}{\eta_{pg}R_{pg}} - \frac{\tau_{pg}}{\eta_{pg}R_{pg}} - T_3 \quad (20)$$

From equations (11) to (19), the torque on the generator pulley is deduced:

$$\tau_{pg} = \frac{\ddot{\theta}_{pg}}{\eta_{pt1}}\left(J_{pt1} + \frac{k_{pt}^2}{\eta_{pt2}}(J_{pt2} + J_{mu} - 2J_{mu}k_{mu}) + \frac{k_{mu}^2(J_{mu} + m_r)}{\eta_{mu}}\right) + \frac{\dot{\theta}_{pg}k_{pt}^2k_{mu}^2}{\eta_{mu}\eta_{pt2}\eta_{pt1}}c_r + \frac{\theta_{pg}k_{pt}^2k_{mu}^2}{\eta_{mu}\eta_{pt2}\eta_{pt1}}k_r \quad (21)$$

For the resistive torque of the generator τ_{mu} (equation 15), its equivalent inertial force, its equivalent rotational damping and its equivalent rotational stiffness, was analyzed and derived previously in [13]:

$$m_r = J_{pg} \quad (22)$$

$$c_r = \frac{K_{re}K_t(R_e + R_i)}{(R_e + R_i)^2 + L_i^2\omega^2} \quad (23)$$

$$k_r = \frac{K_{re}K_tL_i\omega^2}{(R_e + R_i)^2 + L_i^2\omega^2} \quad (24)$$

Taking the data from Table 1 as an example, it can be deduced that the force of inertia of the Dirven Pulley is much lower than the resistant torque of the generator of the Generator Pulley ($J_{pl}\ddot{\theta}_{pl} \ll \tau_{pg}$), thus being able to neglect this term. Therefore the applied force is equal to:

$$F_a = -\frac{J_{pg}\ddot{\theta}_{pg}}{\eta_{pg}R_{pg}} - \frac{\tau_{pg}}{\eta_{pg}R_{pg}} \quad (25)$$

With equation (11) the rotation of the generating pulley θ_{pg} is related to x_1, and with equations (5) and (6) the movement x_1

can be related to x. Giving us the equivalent mechanical system of Figure 5 as a result.

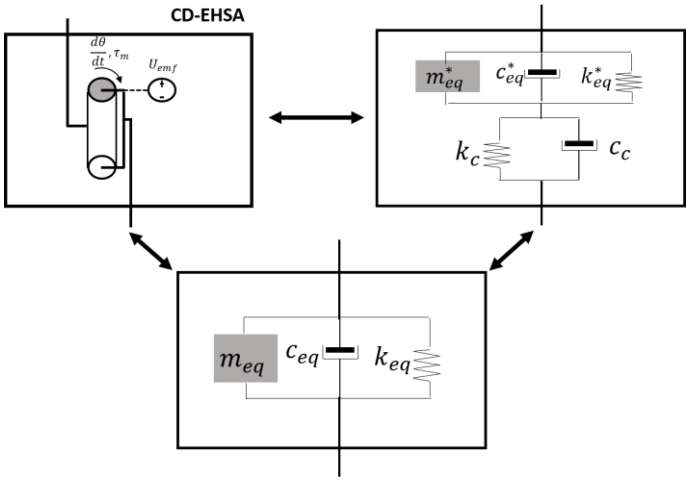

Figure 5. Equivalent mechanical system configuration of the Cable-Dynamics Energy Harvesting Shock Absorber (CD-EHSA).

The equivalent model of the CD-EHSA, mentioned above, may be having a mass, a damper and stiffness in parallel, or a mass, a damper and a different stiffness in series with the stiffness and damping of the cable. For both cases, their values are presented below:

$$m_{eq}^* = \frac{1}{R_{pg}^2 \eta_{pt1} \eta_{pg}} \left(J_{pt1} + J_{pg}\right) + \frac{k_{pt}^2}{R_{pg}^2 \eta_{pt1} \eta_{pg} \eta_{pt2}} \left(J_{pt2} + J_{mu} - 2J_{mu} k_{mu}\right) + \frac{k_{pt}^2 k_{mu}^2}{R_{pg}^2 \eta_{pt1} \eta_{pg} \eta_{pt2} \eta_{mu}} \left(J_{mu} + J_m\right) \quad (26)$$

$$c_{eq}^* = \frac{k_{mu}^2 k_{pt}^2 K_{re} K_t (R_e + R_i)}{R_{pg}^2 \eta_{pt1} \eta_{pg} \eta_{pt2} \eta_{mu} ((R_e + R_i)^2 + L_i^2 \omega^2)} \quad (27)$$

$$k_{eq}^* = \frac{k_{mu}^2 k_{pt}^2 K_{re} K_t L_i \omega^2}{R_{pg}^2 \eta_{pt1} \eta_{pg} \eta_{pt2} \eta_{mu} ((R_e + R_i)^2 + L_i^2 \omega^2)} \quad (28)$$

$$m_{eq} = \frac{\left(m_{eq}^* c_c^2 - {m_{eq}^*}^2 k_c\right)\omega^2 + 2 m_{eq}^* k_{eq}^* k_c}{\left(k_{eq}^* + k_c - m_{eq}^* \omega^2\right)^2 + \left(c_{eq}^* + c_c\right)^2 \omega^2} + \frac{m_{eq}^* k_c^2 - {c_{eq}^*}^2 k_c - k_{eq}^* c_c^2}{\left(k_{eq}^* + k_c - m_{eq}^* \omega^2\right)^2 + \left(c_{eq}^* + c_c\right)^2 \omega^2} \quad (29)$$

$$c_{eq} = \frac{\left({c_{eq}^*}^2 c_c + c_{eq}^* c_c^2 - 2 k_{eq}^* c_c m_{eq}^*\right)\omega^2}{\left(k_{eq}^* + k_c - m_{eq}^* \omega^2\right)^2 + \left(c_{eq}^* + c_c\right)^2 \omega^2} + \frac{{m_{eq}^*}^2 c_c \omega^4 + c_{eq}^* k_c^2 + c_c {k_{eq}^*}^2}{\left(k_{eq}^* + k_c - m_{eq}^* \omega^2\right)^2 + \left(c_{eq}^* + c_c\right)^2 \omega^2} \quad (30)$$

$$k_{eq} = \frac{{k_{eq}^*}^2 k_c + k_{eq}^* k_c^2}{\left(k_{eq}^* + k_c - m_{eq}^* \omega^2\right)^2 + \left(c_{eq}^* + c_c\right)^2 \omega^2} \quad (31)$$

The mathematical model used for the derivation of the equations did not consider so far friction forces. For this reason, in order to obtain a more realistic mathematical model, friction forces are introduced for each of the mobile parts of the system:

$$F_{fr} = f\left(x, \dot{x}, \theta_{pg}, \dot{\theta}_{pg}, \theta_{pt2}, \dot{\theta}_{pt2}, \theta_{mu}, \dot{\theta}_{mu}\right) \quad (32)$$

The friction model used for each of the mobile parts of the system, kinematic pairs, is the one presented by B. Armstrong et al. [30], which is illustrated in Figure 6 and approximated with the following equations:

$$F = \sqrt{2e}(F_{brk} - F_c) \cdot exp\left(-\left(\frac{v}{v_{brk}\sqrt{2}}\right)^2\right) \cdot \frac{v}{v_{st}} + F_c \cdot tanh\left(\frac{10v}{v_{brk}}\right) + f_v \quad (33)$$

$$T = \sqrt{2e}(T_{brk} - T_c) \cdot exp\left(-\left(\frac{\dot{\theta}}{\dot{\theta}_{brk}\sqrt{2}}\right)^2\right) \cdot \frac{\dot{\theta}}{\dot{\theta}_{st}} + T_c \cdot tanh\left(\frac{10\dot{\theta}}{\dot{\theta}_{brk}}\right) + t_v \quad (34)$$

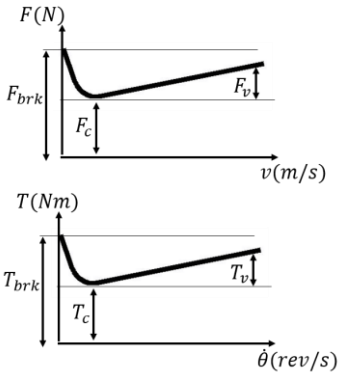

Figure 6. The function of the translational friction (up) and rotational friction (down).

An iterative method was used to determine the numerical values of the friction model, in which, with the help of a multi-objective optimization algorithm (MOOP), the parameters that best fit the experimental results are found.
This done the damping force of the CD-EHSA is finally given by the following expression:

$$F_a = m_{eq}\ddot{x} + c_{eq}\dot{x} + k_{eq}x + F_{fr} \quad (35)$$

IV. LAB TESTS

This section describes both the tests carried out and the results obtained with the CD-EHSA.

A. Experimental Setup

The experimental tests of the CD-EHSA were performed with a MTS 835 machine, as shown in Figure 7. The tests were performed for excitation frequencies between 0.5 and 4 Hz and different electrical resistances (15, 47, 62, 94 and 109). In order to register the voltage signal from the generator, a CompactRio NI cDaq-9178 system was used together with a NI-9234 module.

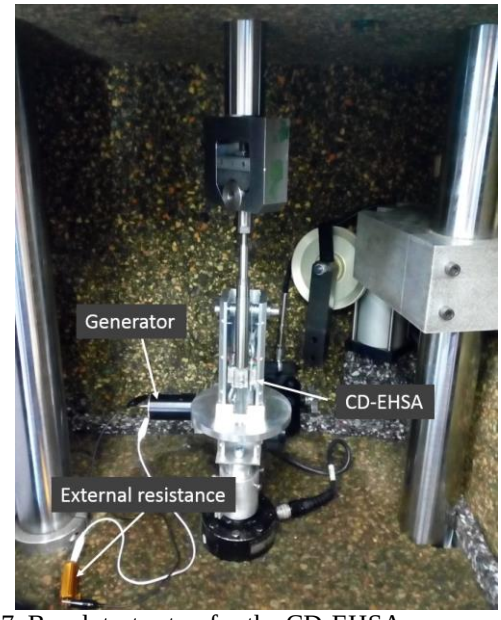

Figure 7. Bench test setup for the CD-EHSA.

When analyzing the results of the tests it could be observed that a slight misalignment between the axis of the multiplier and the generator was producing a vibration at a frequency different form the excitation frequency with which the respective test was performed. It was confirmed that this vibration was due to misalignment, because the frequency of vibration was equal to the product of the multiplication factor of the multiplier (k_{mu}) with the multiplication factor of the transmission pulleys (k_{pt}) by the excitation frequency of the test. Therefore, a *Notch-filter* was applied on the recorded signals in order to attenuate this undesired effect at the frequency where the aforementioned disturbance is present, as shown in Figure 8.

However, the impact of this misalignment in the ride quality could cause the decrease on passenger's comfort and the durability of the mechanism that interview in the system, affecting in the future the feasibility of the CD-EHSA.

Figure 8. Experimental damping force of the CD-EHSA. Top: Frequency domain. Bottom: Time domain.

B. Comparison of simulations and experiments.

For the simulation of the behavior of the CD-EHSA, the Simscape/Mathworks program is used, which uses the mathematical equations derived in the previous section.

The simulation results together with the experimental ones can be observed in Figure 9. They show that the computational model created captures the main characteristics of the experimental results of both the excitation force and the generated voltage.

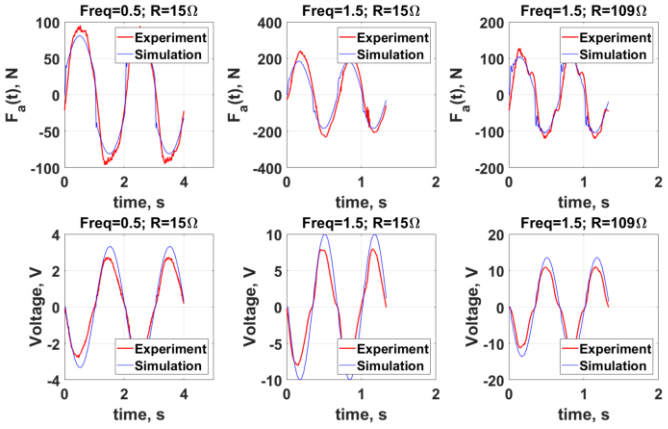

Figure 9. Simulation and experimental results of the CD-EHSA at different excitation frequencies and external load. Top: Damping force. Bottom: Generator voltage

C. Force-displacement loops, damping characteristics and harvesting power.

The prototype was tested, as indicated above, at different excitation frequencies and varying external resistances. The force-displacement graphs can be seen in Figure 10 and Figure 11.

Figure 10 shows the force-displacement ellipsoid of the CD-EHSA at different excitation frequencies. The area of the ellipsoid represents the energy dissipated+recovered from the damper. Clearly this energy is higher when the frequency is increased.

Figure 11 shows, likewise, the force-displacement ellipsoid but varying the electrical resistance connected to the generator. As can be seen the dissipated+recovered energy increases as the impedance value decreases.

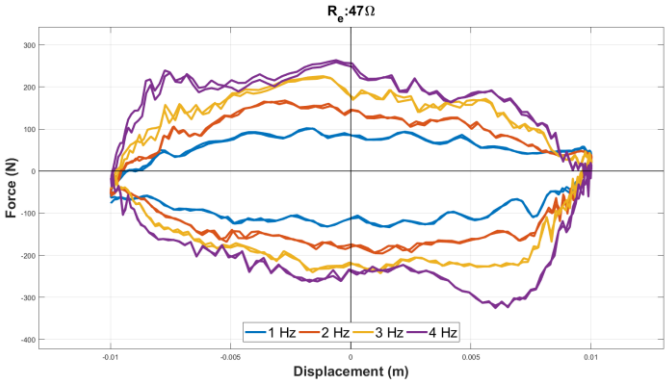

Figure 10. Force-displacement loop for different frequencies with 47Ω external load and 15 mm displacement input.

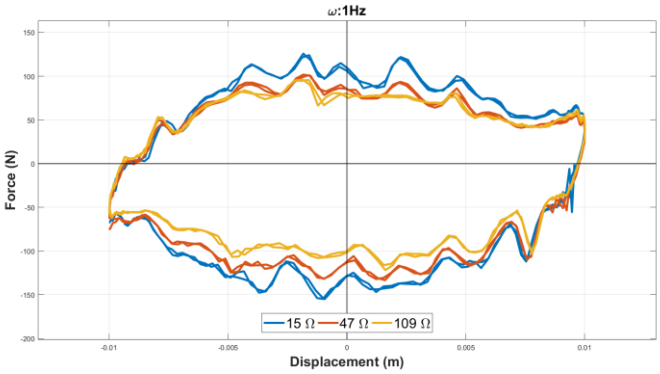

Figure 11. Force-displacement loops for different electrical loads at displacement input of 1Hz and 15 mm amplitude.

Figure 12 shows the relationship between force and speed. This image shows that there is linearity between the two variables and its slope, which corresponds to the damping coefficient c_{eq}, and that it depends on the electrical resistance that is connected to the generator. The higher the resistance, the lower the slope and vice versa. In the image we can observe the phase difference φ that exists between the slopes with the resistances of 15 Ω and 109 Ω.

Figure 13 shows the instantaneous electrical power to different connected electrical resistances. This power was obtained using the voltage and the value of the resistance, $P_{out} = {V^2}/{R_e}$. Obtaining peak values of 1.4 W and 0.5 W for resistances of 15Ω and 109Ω.

The mechanical efficiency ranges from 4% to 22% with different vibration frequencies (see Figure 14) and different electrical loads. It is important to remark that the mechanical efficiency shown at Figure 14, is from experimental data and it is defined as:

$$\eta_g^e = \frac{{V_g^e}^2/R_e}{(F_a^e)\dot{x}} \tag{36}$$

Where the numerator is the experimental electric power generated and the denominator is the damped power, which is composed by the experimental input force of the CD-EHSA (equation 35) multiplied by the experimental input velocity recorded by the bench test.

In spite of having filtered the vibrations coming from the misalignment between the generator and the multiplier, there are other fluctuations in the signals originated from the imperfections between the couplings of the moving parts. This problem can be improved as tolerance values are adjusted when the CD-EHSA is manufactured and assembled.

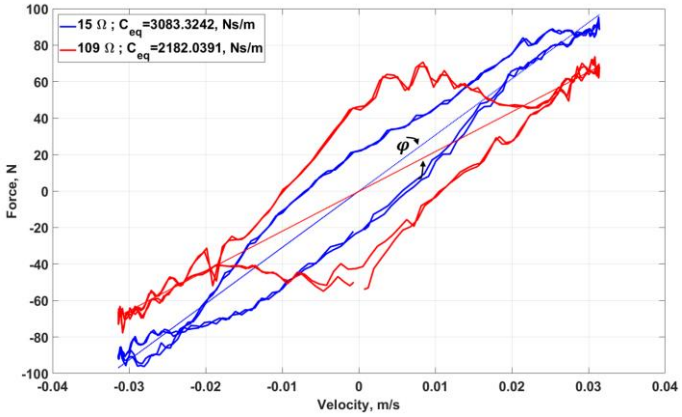

Figure 12. Force-velocity for different electrical loads at displacement input of 0.5 Hz frequency and 10 mm amplitude.

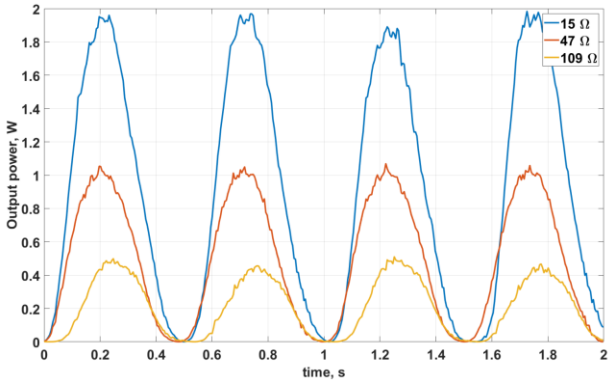

Figure 13. Output electrical power for different electrical loads at displacement input of 1 Hz frequency and 15 mm amplitude.

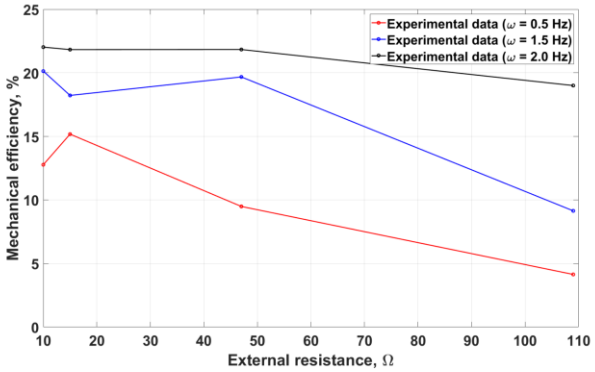

Figure 14. Electromechanical conversion efficiency of the energy- harvesting damper including the mechanical and electrical efficiencies, which are calculated as the output electrical power generated divided by the damped power, at different excitation frequencies.

V. ROAD TESTS AND PERFORMANCES

This section shows some results of the energy recovery potential of the CD-EHSA system. Test have been carried out on a Renault Twizy 45 car, in order to obtain the relative displacements of its 4 shock absorbers when driving in a circuit at a certain speed. Using these data and with the characteristic curves of the dampers of the vehicle itself, the power that can be recovered with the CD-EHSAs is calculated.

The trajectory that was followed within the University campus at a speed between 20-30 Km/h, is indicated in Figure 15.b). Cable extension transducers (POSIWIRE®), were used for the instrumentation of the vehicle, together with the cDaq NI cDaq-9178 equipment and the NI-9234 module for data acquisition, shown in Figure 15 (right). At the moment, our research is focused on low-speed damped which is why the circuit have been done at low velocity.

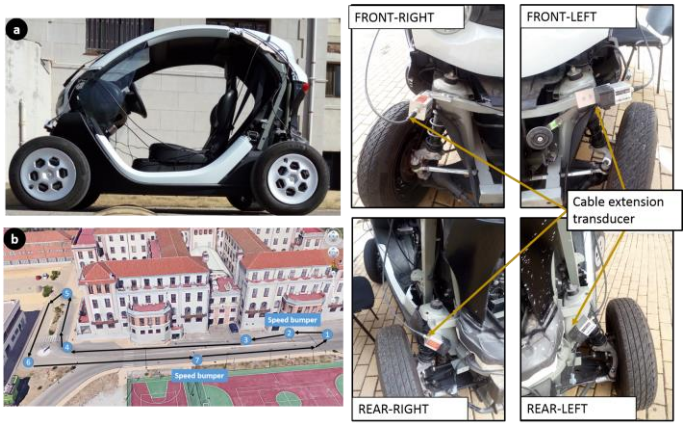

Figure 15. Left: a) Renault Twizy and b) Trajectory followed in the experiment. Right: Mounting sensors on the suspensions.

Figure 16 shows the relative displacement between the ends of the four suspensions. These data are used as input signals in the computational model created for the CD-EHSA.

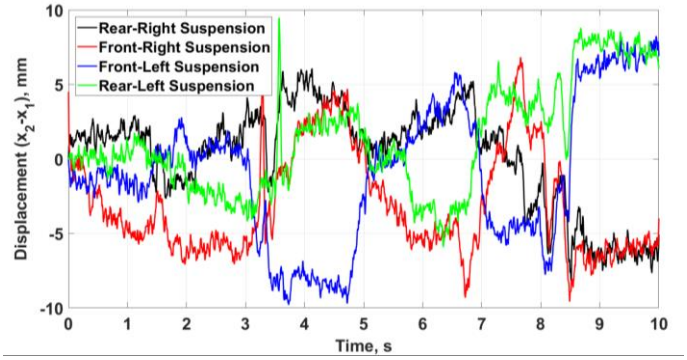

Figure 16. Suspension displacement between the ends from all four shock absorbers, recorded on a local circuit at 20-30 Km/h.

Each of the energy recovery dampers has been designed to have the same force-velocity characteristics curves as the actual Renault Twizy dampers (see Figure 17). The characteristics curves of the Renault Twizy shock absorbers were obtained from the MTS 835 machine.

The damping value c_{eq} of the CD-EHSA is adjusted by varying the external resistance connected to the generator. By means of a diode circuit it is possible to obtain different slopes both in compression and extension, imitating the behavior found in hydraulic shock absorbers.

Table 2 shows the different damping values c_{eq} that can be achieved for different resistance values. It is important to remark that the values that appear in Table 2 correspond to theoretical damping values (c_{eq}), they don't take into account the nonlinear friction parameters. That is why the damping values are shown in Figure 12 are higher than shown in Table 2. The purpose of show the different damping values, for different external loads, at Table 2 is to illustrate how the theoretical EHSA behave at different conditions. Values of equivalent damping, with external resistance greater than 100 Ω do not change considerably, and less than 2 Ω are very difficult to obtained because of the own electrical impedance from the cables that connect the generator with resistance.

Table 2. Different values of c_{eq}, depending on the external load.

External Resistance R_e (Ω)	Equivalent Damping value c_{eq} $(N/(m/s))$
2	2720
10	1405
25	738
100	220

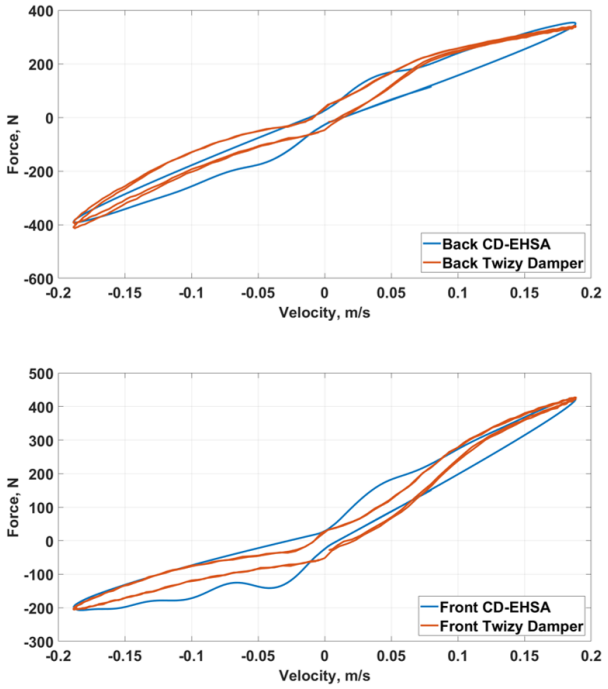

Figure 17. Force-velocity curve from the CD-EHSA and the Twizy's dampers. Top: Shock absorbers at the back. Bottom: Shock absorbers at the front.

The installation of CD-EHSA is simulated for each suspension (Figure 18), the results show that a total average power of 105W can be obtained, having peaks of power of 400-500 W when passing through speed bumps (Figure 19).
The instantaneous power generated, showed at Figure 19, is adjusting the external resistance to have the same force-speed curve as in the Renault Twizy dampers. However, Figure 20 shows the RMS power generated with different resistances and different driver speed, using the relative displacement data from the suspension at the back and front. The figure shows how the increase of the resistance, decrease the value of power generated, and at higher driver speed the greater the power recovered.

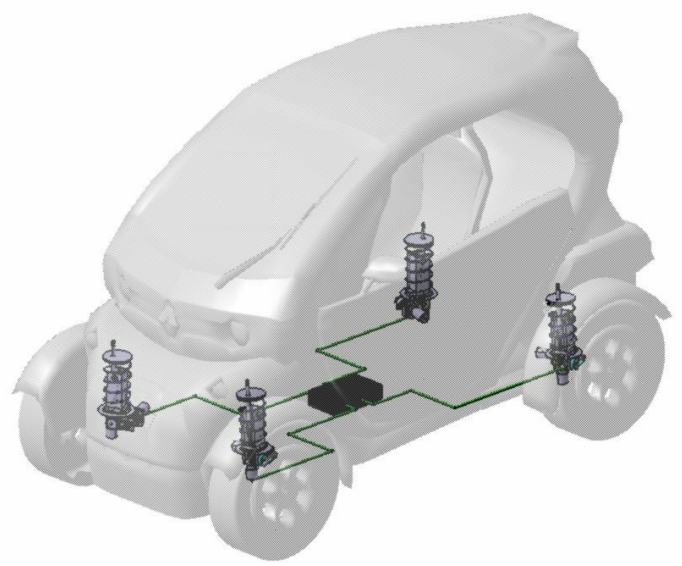

Figure 18. Application of the Cable-Dynamics Energy Harvesting Shock Absorbers (CD-EHSA) in range extended EVs

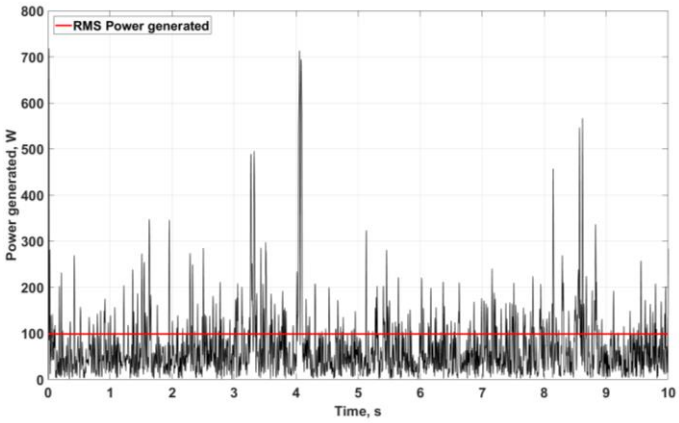

Figure 19. The road test results of output electrical power from the four shock absorbers at 20-30 Km/h. The red line means the RMS Power generated.

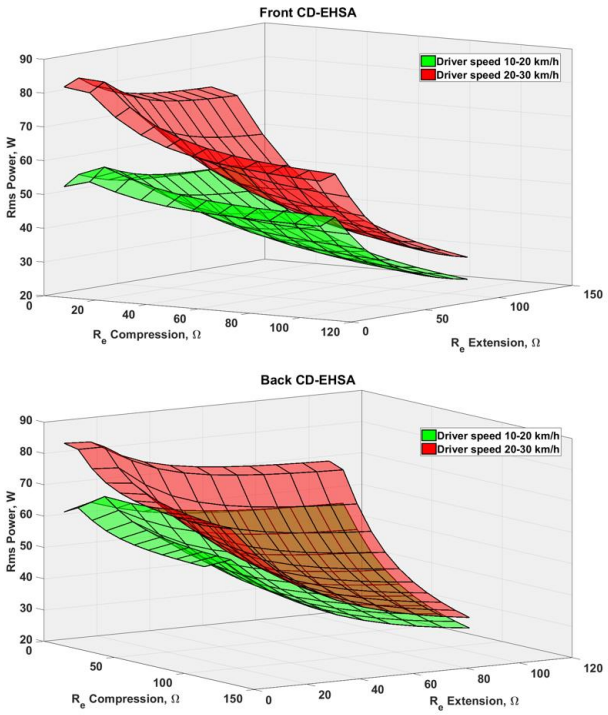

Figure 20. RMS electrical power generated by the CD-EHSA at different driver speed and different resistances. Top: Using the relative displacement from the Twizy front suspension. Bottom: Using the relative displacement from the Twizy back suspension.

With the resistance values adjusted to have the same force-speed curve as in the Renault Twizy dampers, the mechanical efficiency of the system is around 26%. However, by varying the values of the damping coefficient (e.g. changing the external load), the CD-EHSA system can reach an efficiency of more than 60%, see Figure 21. The efficiency (ηg) of the CD-EHSA, represents the amount of energy that is "recovered" with respect to the energy that is used to damp. For that reason it is composed of the electric power divided by the damped power. It is defined as:

$$\eta_g = \frac{V_g^2/R_e}{(F_a - m_{eq}\ddot{x} - k_{eq}x)\dot{x}} \qquad (37)$$

Where the numerator is the electric power generated, which is composed of the voltage on the generator V_g squared, divided by the electric resistance R_e. On the other hand, the denominator, the damped power, is composed by the damping force of the CD-EHSA (equation 35) multiplied by the relative velocity between the non-suspended mass and suspended mass, not taking account the inertial and the stiffness force inherent to the CD-EHSA.

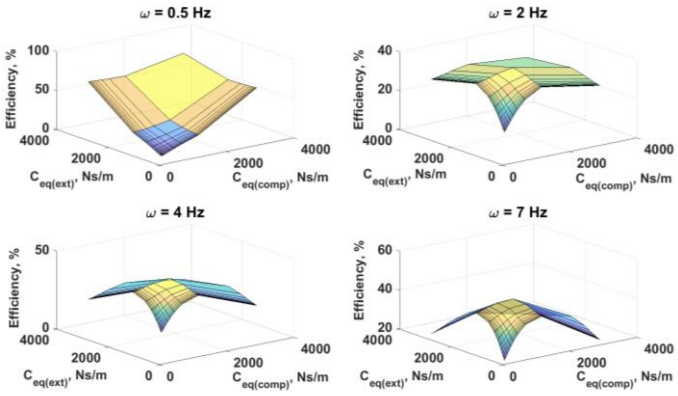

Figure 21. Efficiencies of the CD-EHSA under different damping coefficient (for extension and compression), varying the external load R_e. The graph plots at different excitation frequencies and vibration amplitude of 10 mm.

Figure 21 shows that the energy efficiency decreased, at high damping coefficient, conforming the excitation frequency increases. And also, that the optimal efficiency, when the excitation frequency is upper 2Hz, is when the damping coefficient is between 900-1100 Ns/m.

VI. CONCLUSIONS

This article presents an innovative system for energy recovery in vehicle dampers. This type of Energy Harvesting Shock Absorber uses a cable transmission (called CD-EHSA) to convert the movement of translation -found in most of the conventional dampers- to a rotation which is more adaptable to the shaft of a conventional generator. With this type of transmission, inertias and backlash when the direction of travel changes are reduced. However, despite the fact that the backslash decreases when the pre-tension of the cable is increased it is necessary to take special care as the bearings are directly affected.

The modelling shows that the CD-EHSA's damping force can be subdivided in four forces, the friction forces and one related to the damping forces, other related to the stiffness forces and the last related to the inertias forces from the moving parts. The last three forces, in comparison to other EHSAs models from the literature depends more in the excitation frequency, having an EHSA more sensible for high frequencies.

The prototype is also evaluated on a testing machine, MTS 835, with sinusoidal displacement input. The experimental results shows that the friction forces affect in strong way to the resulting damping coefficient. Having to take in consideration for its design to a specific car.

Additionally, tests have been conducted on a Renault Twizy 45, instrumented in order to obtain actual relative displacement in the suspensions on a specific road test. With this data and with the characteristic curve of the dampers of the chosen vehicle, an estimation of the electric power that such a system can generate was obtained. The results shows that a mean square power of 105W, driving at a speed between 20-30

Km/h, is achieved. With power peaks, when passing through a speed bump, of 400-500 W.

The efficiency of the system varies depending of the electrical resistance that is connected to it. By means of a diode circuit it is possible to have different damping values depending on the state of the damper. With a resistance of 25Ω for extension and 20Ω for compression the system can have an efficiency of around 60%. In the design of the EHSA, there is the decision to make between, prioritize the energy efficiency or the damping force need. A systematic analysis of interaction between energy efficiency, ride comfort and rode handling will be conducted in the future.

The advantage of the electromagnetic EHSAs is that their damping values can be adjusted by changing the electrical resistance. Giving rise, as a new line of research, to be able to develop a semi active EHSA, i.e. with a variable resistance that allows to control at all times the adequate damping.

Another future lines is going on an improved mechanical design of the CD-EHSA in which the weight, inertias and friction are reduced. Even though this kind of transmission has been used in applications with high dynamical force, and different values of excitation frequency, the analysis in the suspension dynamics is still premature. However, the authors considered this kind of transmission as a valuable technology to improve EHSA performance.

ACKNOWLEDGMENT

The authors wish to thank the financial support provided by the Spanish Ministry of Economy and Competiveness by the financial support to the Project POWER Ref. ENE2014-57043-R and *Cátedra Global Santander-Nebrija en Tecnologías para el Transporte Sostenible*.

REFERENCES

[1] F. Chiara and M. Canova, "A review of energy consumption, management, and recovery in automotive systems, with considerations of future trends," *Proc. Inst. Mech. Eng. Part D J. Automob. Eng.*, vol. 227, no. 6, pp. 914–936, 2013.

[2] P. Z. T. Decoupler, "Vibration energy harvesting from a hydraulic engine mount via PZT decoupler," in *Proceeding of the ASME 2010 International Mechanical Engineering Congress & Exposition IMECE2010*, 2010.

[3] J. Lee and B. Choi, "Development of a piezoelectric energy harvesting system for implementing wireless sensors on the tires," *Energy Convers. Manag.*, vol. 78, pp. 32–38, 2014.

[4] X. D. Xie and Q. Wang, "Energy harvesting from a vehicle suspension system," *Energy*, vol. 86, pp. 385–392, 2015.

[5] H.-X. Zou, W.-M. Zhang, K.-X. Wei, W.-B. Li, Z.-K. Peng, and G. Meng, "Design and Analysis of a Piezoelectric Vibration Energy Harvester Using Rolling Mechanism," *J. Vib. Acoust.*, vol. 138, no. 5, p. 051007, 2016.

[6] M. A. A. Abdelkareem, L. Xu, M. K. A. Ali, A. Elagouz, J. Mi, S. Guo, Y. Liu, and L. Zuo, "Vibration energy harvesting in automotive suspension system: A detailed review," *Appl. Energy*, vol. 229, no. August, pp. 672–699, 2018.

[7] E. Asadi, R. Ribeiro, M. B. Khamesee, and A. Khajepour, "Analysis, prototyping, and experimental characterization of an adaptive hybrid electromagnetic damper for automotive suspension systems," *IEEE Trans. Veh. Technol.*, vol. 66, no. 5, pp. 3703–3713, 2017.

[8] X. Tang, T. Lin, and L. Zuo, "Design and optimization of a tubular linear electromagnetic vibration energy harvester," *IEEE/ASME Trans. Mechatronics*, vol. 19, no. 2, pp. 615–622, 2014.

[9] L. Zuo, B. Scully, J. Shestani, and Y. Zhou, "Design and characterization of an electromagnetic energy harvester for vehicle suspensions," *Smart Mater. Struct.*, vol. 19, no. 4, p. 045003, 2010.

[10] G. Zhang, J. Cao, and F. Yu, "Design of active and energy-regenerative controllers for DC-motor-based suspension," *Mechatronics*, vol. 22, no. 8, pp. 1124–1134, 2012.

[11] B. Huang, C. Y. Hsieh, F. Golnaraghi, and M. Moallem, "Development and optimization of an energy-regenerative suspension system under stochastic road excitation," *J. Sound Vib.*, vol. 357, pp. 16–34, 2015.

[12] W. Salman, L. Qi, X. Zhu, H. Pan, X. Zhang, and S. Bano, "A high-efficiency energy regenerative shock absorber using helical gears for powering low-wattage electrical device of electric vehicles A high-ef fi ciency energy regenerative shock absorber using helical gears for powering low-wattage electrical device ," *Energy*, vol. 159, no. June, pp. 361–372, 2018.

[13] Z. Li, L. Zuo, G. Luhrs, L. Lin, and Y. Qin, "Electromagnetic Energy-Harvesting Shock Absorbers: Design, Modeling, and Road Tests," *IEEE Trans. Veh. Technol.*, vol. 62, no. 3, pp. 1065–1074, Mar. 2013.

[14] Z. Li, L. Zuo, J. Kuang, and G. Luhrs, "Energy-Harvesting Shock Absorber with a Mechanical Motion Rectifier," *Smart Mater. Struct.*, pp. 1–15, 2012.

[15] S. Guo, Y. Liu, L. Xu, X. Guo, and L. Zuo, "Performance evaluation and parameter sensitivity of energy-harvesting shock absorbers on different vehicles," *Veh. Syst. Dyn.*, vol. 54, no. 7, pp. 918–942, 2016.

[16] Z. Zhang, X. Zhang, W. Chen, Y. Rasim, W. Salman, H. Pan, Y. Yuan, and C. Wang, "A high-efficiency energy regenerative shock absorber using supercapacitors for renewable energy applications in range extended electric vehicle," *Appl. Energy*, vol. 178, pp. 177–188, 2016.

[17] S. N. Avadhany, "Analysis of Hydraulic Power Transduction in Regenerative Rotary Shock Absorbers as Function of Working Fluid Kinematic Viscosity," Massachusetts Institute of Technology, 2009.

[18] Y. Zhang, X. Zhang, M. Zhan, K. Guo, F. Zhao, and Z. Liu, "Study on a novel hydraulic pumping regenerative suspension for vehicles," *J. Franklin Inst.*, vol. 352, no. 2, pp. 485–499, 2015.

[19] J. Zou, X. Guo, L. Xu, G. Tan, C. Zhang, and J. Zhang, "Design, Modeling, and Analysis of a Novel Hydraulic Energy-Regenerative Shock Absorber for Vehicle Suspension," *Shock Vib.*, vol. 2017, pp. 1–12, 2017.

[20] M. A. A. Abdelkareem, L. Xu, X. Guo, M. K. A. Ali, A. Elagouz, M. A. Hassan, F. A. Essa, and J. Zou, "Energy harvesting sensitivity analysis and assessment of the potential power and full car dynamics for different road modes," *Mech. Syst. Signal Process.*, vol. 110, no. March, pp. 307–332, 2018.

[21] R. Sabzehgar, A. Maravandi, and M. Moallem, "Energy Regenerative Suspension Using an Algebraic Screw Linkage Mechanism," *IEEE/ASME Trans. Mechatronics*, vol. 19, no. 4, pp. 1251–1259, 2013.

[22] A. Maravandi and M. Moallem, "Regenerative shock absorber using a two-leg motion conversion mechanism," *IEEE/ASME Trans. Mechatronics*, vol. 20, no. 6, pp. 2853–2861, 2015.

[23] R. Zhang, X. Wang, E. Al Shami, S. John, L. Zuo, and C. H. Wang, "A novel indirect-drive regenerative shock absorber for energy harvesting and comparison with a conventional direct-drive regenerative shock absorber," *Appl. Energy*, vol. 229, no. July, pp. 111–127, 2018.

[24] Y. Jung and J. Bae, "An asymmetric cable-driven mechanism for force control of exoskeleton systems," *Mechatronics*, vol. 40, pp. 41–50, 2016.

[25] J. Savall, "Diseño Mecánico de Dispositivos Hápticos de Gran

Espacio de Trabajo : Aplicación al Sector Aeronáutico," Universidad de Navarra, 2005.

[26] J. Savall, J. Martín, and A. Avello, "High-Performance Linear Cable Transmission," *J. Mech. Des.*, vol. 130, no. 6, p. 064501, 2008.

[27] Y. Lu, D. Fan, H. Liu, and M. Hei, "Transmission capability of precise cable drive including bending rigidity," *Mech. Mach. Theory*, vol. 94, pp. 132–140, 2015.

[28] Y. Liu, L. Xu, and L. Zuo, "Design, Modeling, Lab and Field Tests of a Mechanical-motion-rectifier-based Energy Harvester Using a Ball-screw Mechanism," *IEEE/ASME Trans. Mechatronics*, vol. 22, no. 5, pp. 1933–1943, 2017.

[29] Z. Li, Z. Brindak, and L. Zuo, "Modeling of an Electromagnetic Vibration Energy Harvester With Motion Magnification," *ASME 2011 Int. Mech. Eng. Congr. Expo.*, no. June, pp. 285–293, 2011.

[30] B. Armstrong and C. C. de Wit, "Friction Modeling and Compensation," in *The Control Handbook*, CRC Press, 1995.

Lincoln Bowen

First author. Received his B.S. and M.S. degree in Industrial Engineering from University of Navarra, San Sebastian – Spain in 2013. He is now working toward his Ph.D. degree in mechatronic engineer at University of Nebrija. Lincoln's research includes innovative shock absorber, vehicle dynamics, energy harvesting, and vibration control.

Jordi Viñolas

Received his Industrial Engineering and PhD. Degrees from the University of Navarra in San Sebastian - Spain.

At present Dean and professor of the School of Engineering and Architecture at Universidad Antonio de Nebrija. Previously Head of European Projects at Bantec, a consulting pioneer in the integrated R&D management,for companies, scientific-technological agents and government. His scientific interests have focused on the fields of machine dynamics, noise and vibration, railway dynamics and road infrastructure. He has published around 50 indexed (JCR) scientific papers and 40 communications in International/National Conferences.

José Luis Olazagoitia

Received his Industrial Engineering (Mechanics Intensification) and the PhD. Degrees from the University of Navarra in San Sebastian - Spain. He is professor of "Machine Calculation, Design and Testing" at the Nebrija University. His PhD. Work (1999) was focused on Optimization Techniques applied to the design of mechanisms. He is currently working on advanced active safety and vehicle dynamics within the research group of Automotive Engineering.

Javier Echávarri Otero

Javier Echávarri Otero received the Mechanical Engineer degree in 2000 at the Universidad Politécnica de Madrid. At the same University he received a Ph.D. degree cum laude in Mechanical Engineering in 2005. He teaches "Theory of Machines and Mechanisms", "Machine Design" and "Tribology" at Universidad Politécnica de Madrid. He is technical head of the Machines and Mechanisms Lab. His research interests are in the area of Mechanical Engineering, including Tribology and Safety in Machinery.